Thermochimica Acta 513 (2011) 106–111

Contents lists available at ScienceDirect

Thermochimica Acta

journal homepage: www.elsevier.com/locate/tca

Heat flow calorimetry and SEM investigations to characterize the hydration at different temperatures of different $12CaO{\cdot}Al_2O_3$ ($C_{12}A_7$) samples synthesized by solid state reaction, polymer precursor process and glycine nitrate process

B. Raab*, H. Poellmann

Mineralogy and Geochemistry, Institute of Geological Sciences, Martin-Luther-University Halle-Wittenberg, Von-Seckendorff-Platz 3, 06108 Halle, Germany

ARTICLE INFO

Article history:
Received 4 August 2010
Received in revised form 8 November 2010
Accepted 9 November 2010
Available online 23 November 2010

Keywords:
$C_{12}A_7$
Mayenite
C_5A_3
Hydration
Polymer precursor synthesis
Glycine nitrate process
Heat flow calorimetry

ABSTRACT

Mayenite was synthesized using the conventional solid-state reaction and two low temperature synthesis methods a self-combustion method and a polymeric precursor process. Using the low temperature methods the metastable phase $5CaO{\cdot}3Al_2O_3$ (C_5A_3) crystallizes at 1173 K (2 h) instead of $C_{12}A_7$. After forming pure crystalline $12CaO{\cdot}7Al_2O_3$ ($C_{12}A_7$) at 1373 K (2 h) the hydration was monitored at 283 K, 288 K, 293 K, 298 K and 301 K by heat flow calorimetry. During hydration the first calorimetric peak correlates with the formation of layers around the $C_{12}A_7$ grains and the second peak corresponds to further hydration reactions and crystallization of lamellar calcium aluminate hydrates $C_2AH_{8\pm x}$ showing different hydration steps of $8.2H_2O$, $8.0H_2O$ and $7.5H_2O$ depending on temperature. At higher temperatures the formation of hydrate shells is increased and consequently the further hydration reaction is hindered.

1. Introduction

The phase compositions of calcium aluminate clinkers are quite complex [1,2]. In order to understand the hydration behaviour of Mayenite ($C_{12}A_7$) it was synthesized using solid state reactions and low temperature synthesis methods. As precursors for the synthesis of $C_{12}A_7$ using solid state reaction, stoichiometric amounts of CaO (C) and Al_2O_3 (A) were required. To get pure phases without any additional phases, long sintering intervals at higher temperatures with a few intermediate grinding steps are needed. The formation of pure phases can be accelerated by the use of pressed powder pellets from the precursor powder. This corresponds with lower specific surfaces after the sintering process, thus more intensive grinding is needed. Therefore low temperature techniques are used, to synthesize the pure phases much faster by getting more homogeneous precursor phases. According to the literature [3] different sol–gel, self-combustion and polymeric precursor methods are used, but the crystallization process and hydraulic reactivity were not sufficiently studied. The sol–gel method is an alternative way to mix precursor phases very homogenously. Consequently the method was also used to produce glasses and ceramics at low temperatures. Amorphous calcium aluminate glasses were produced by Goktas and Weinberg [4] and Kerns et al. [5] with the sol–gel method. They used calcium-*sec*-butylate ($Al(OC_4H_9)_3$) and calcium nitrate hydrate ($Ca(NO_3)_2{\cdot}4H_2O$) as precursor phases. The disadvantage of this method is the long gelation time of up to 3–6 days. Stephan and Wilhelm [6] used a commercial Al_2O_3-sol and $Ca(NO_3)_2{\cdot}4H_2O$ to synthesize several calcium aluminates, at temperatures up to 1773 °C, in order to produce pure monocalcium aluminate.

The self propagating combustion synthesis (SPCS) is a synthesis method of metal oxides. This method uses an oxidant (e.g. metal nitrates) and a fuel (e.g. glycine, urea or citric acid) as precursor phases dissolved in water [7]. After gelation and thermal activation, the exothermal combustion reaction takes place. Tas [8] synthesized different calcium aluminates with urea as fuel. Hwang et al. [7] showed the influences of different fuels (glycine, urea and citric acid) and the fuel-to-oxidant ratios. In cases, when glycine is used as a fuel, the method is also called glycine nitrate process (GNP) [9–14].

As an alternative method to sol–gel method and SPCS, the polymeric precursor processes were applied for synthesis also. Among these techniques the Pechini-type polymerized complex method is well known. Kakali et al. [15], Gaki et al. [16,17] and Hong and Young [18] used citric acid and ethylene glycol to form a polymeric resin, which contains the relevant ions. Lee and Kim [19], Lee and

* Corresponding author. Tel.: +49 345 5526164; fax: +49 345 5527180.
E-mail addresses: bastian.raab@geo.uni-halle.de (B. Raab), herbert.poellmann@geo.uni-halle.de (H. Poellmann).

0040-6031/$ – see front matter © 2010 Elsevier B.V. All rights reserved.
doi:10.1016/j.tca.2010.11.019

Lee [20] and Chai et al. [21] showed that the amount of resin and the molecular weight have an influence on the crystallization process.

Additionally it is possible to synthesize calcium aluminates at lower temperatures by the decomposition of stoichiometric solutions of metal-nitrates, -chlorides or -carboxylates. This method has the disadvantage, that a very fast drying process of the solution is necessary for example by a spray pyrolysis process. This method was successfully used by Douy and Gervais [22] to synthesize calcium aluminates. However, the construction of an apparatus for such a system is complicated and expensive.

The hydration behaviour of $C_{12}A_7$ was investigated by Edmonds and Majumdar [23] at different temperatures. Besides the amorphous phase, just a small content of crystalline hydration products was formed. Below 293 K, the crystalline phases $2CaO{\cdot}Al_2O_3{\cdot}8H_2O$ (C_2AH_8) and $CaO{\cdot}Al_2O_3{\cdot}10H_2O$ (CAH_{10}) occur. Between 293 K and 301 K just C_2AH_8 occurs and above 301 K the conversion into stable hydrogarnet $3CaO{\cdot}Al_2O_3{\cdot}6H_2O$ (C_3AH_6) and gibbsite $Al(OH)_3$ is accelerated. The reaction at 293 K is delayed, compared to 277 K or 313 K, because of the nucleation of phases at 293 K. Qijun et al. [24] investigated the hydration behaviour of the compound $11CaO{\cdot}7Al_2O_3{\cdot}CaF_2$ and described the degree of hydration to be low at 288 K at the beginning of the hydration, which increases with hydration process. At higher temperatures (303 K, 313 K and 333 K) the degree of hydration is increased at the beginning, but decreases strongly with hydration process. Qijun et al. [24] supposed that at lower temperatures porous layers of the first hydration products were built around the $C_{12}A_7$ grains because of lower solubility at low temperatures. At higher temperatures layers are much denser and the further hydration is hindered. You et al. [25] showed the influence of the crystallinity of $C_{12}A_7$ to the hydration behaviour. They measured, that amorphous $C_{12}A_7$ is more reactive at the beginning of hydration but at later times the reactivity is lower compared to crystalline $C_{12}A_7$. You et al. [25] concluded that the higher solubility at early times for amorphous $C_{12}A_7$ form denser layers around the $C_{12}A_7$ grains and further hydration is consequently hindered.

In this investigation a comparison of the formation of $C_{12}A_7$ with different synthesis methods is made. Additionally the hydraulic reactivity of $C_{12}A_7$ produced by these synthesis methods was studied. The measurements of hydration were performed in the temperature range from 283 K to 301 K.

2. Experimentals

2.1. Characterization methods

The powders were investigated by X-ray diffraction using a PANalytical diffractometer (X-Pert MPD), $Cu_{K\alpha}$-radiation (45 kV, 40 mA), automatic slits and X'Celerator detector. Scanning electron microscopy (LEO 1530VP) was applied to visualize the morphology of pure phases and hydration products. The hydrated phases were prepared by a Gatan Alto 2500 cryo-transfer unit to avoid dehydration effects of hydrate phases under high vacuum [26]. The heat flow calorimeter used for this study consists of an aluminium block which is situated in an isolated box. It is equipped with a quadrupled layout of Bi/Te semiconductor measurement cells (three sample cells + reference cell) [27]. The calorimeter runs in an isoperibolic mode using a temperature control unit by MESICON. The $C_{12}A_7$ powder (1 g) was weighted into copper crucibles which were closed tightly and sited into the calorimeter. The water was added by a modified injection method at different temperatures after equilibration [28]. The measurement was performed in a differential mode comparing the temperature difference between copper vessels with $C_{12}A_7$ paste to an empty copper vessel as reference. The specific surface was measured by BLAINE (DIN EN 196-6) and N_2 adsorption according to the BET method described by Brunauer et al. [29]. By sintering the precursor phases produced by the different methods a heating rate of 10 K/min was applied. After the sintering steps, the samples were quenched in air.

2.2. Synthesis

2.2.1. Solid-state reaction

CaO and alpha-Al_2O_3 (p.a., Fluka Chemie AG, Ulm/Germany) were mixed in stoichiometric ratios to get pure $C_{12}A_7$. CaO was produced by the decomposition of $CaCO_3$ (p.a., Fluka Chemie AG, Ulm/Germany) for 1 h at 1273 K.

2.2.2. Glycine nitrate process (GNP)

Starting powders of $Ca(NO_3)_2{\cdot}4H_2O$ (p.a., AppliChem GmbH, Darmstadt/Germany) and $Al(NO_3)_3{\cdot}9H_2O$ (p.a., Sigma–Aldrich Laborchemikalien GmbH, Hohenbrunn/Germany) were weighed in corresponding amounts ($Ca(NO_3)_2{\cdot}4H_2O/Al(NO_3)_3{\cdot}9H_2O$ ratio = 12/14) and were dissolved in deionised water at room temperature to yield a solution of 1 mol/dm^{-3}. Glycine $C_2H_5N_2O$ (p.a., AppliChem GmbH, Darmstadt/Germany) was added to the solution and stirred for 1 h at room temperature (molar ratio: glycine/metal cations = 1.5). After drying the mixture at 443 K, it was heated to 523 K till the exothermic reaction takes place [7]. The combustion reaction took place within a few minutes and a foamy and voluminous precursor powder was formed. These powders can be heated to get crystalline phases.

2.2.3. Pechini process

Pure $Ca(NO_3)_2{\cdot}4H_2O$ (p.a., AppliChem GmbH, Darmstadt/Germany) and $Al(NO_3)_3{\cdot}9H_2O$ (p.a., Sigma–Aldrich Laborchemikalien GmbH, Hohenbrunn/Germany) were used as source materials for CaO and Al_2O_3. In the first step, citric acid $C_6H_8O_7$ (p.a., AppliChem GmbH, Darmstadt/Germany) was dissolved in deionised water. Metal nitrates were added in defined amounts. The solution was stirred and heated to 333 K (molar ratio: citric acid/metal cations = 1). Next ethylene glycol $C_2H_6O_2$ (p.a., AppliChem GmbH, Darmstadt/Germany) was added (molar ratio: ethylene glycol/citric acid = 2) and the solution was stirred at 373 K to obtain a viscous gel. This gel was dried at 423 K in a drier and very voluminous foam was obtained. This foam was crushed and used as precursor phases for sintering.

3. Results and discussion

3.1. Phase formation

The starting powders of solid state reaction were mixed and sintered five times with intermediate grinding steps and a maximum temperature of 1573 K (4 h) to obtain pure $C_{12}A_7$. As minor phases, CA and C_3A occurred during this sintering process. The precursor powder, synthesized by the GNP is X-ray amorphous (Figs. 1a and 2). In sintering processes the powder was heated step by step. At a sintering step of 2 h at 1073 K the foamy precursor starts to crystallize. In the X-ray pattern a wide amorphous peak at about 31° 2θ occurs (Fig. 1b) at this sintering step. The peak has the same position as the two main peaks of the metastable phase $5CaO{\cdot}3Al_2O_3$ (C_5A_3). The unit cell and structure of C_5A_3 was determined by Aruja [30] and Vincent and Jeffery [31]. In Fig. 3 the SEM images show that at this sintering step small particles of 50 nm are formed out of the amorphous foam. Sintering the precursor powder 2 h at 1173 K, C_5A_3 plus small amounts of $3CaO{\cdot}Al_2O_3$ (C_3A) crystallize (Fig. 1c). Agglomerated particles with a size of about 50 nm can be seen at this sintering temperature in the SEM image (Fig. 4). From X-ray pattern (Fig. 1c) the crystallite size was measured using the integrated full with of half maximum [32]. The calculation was

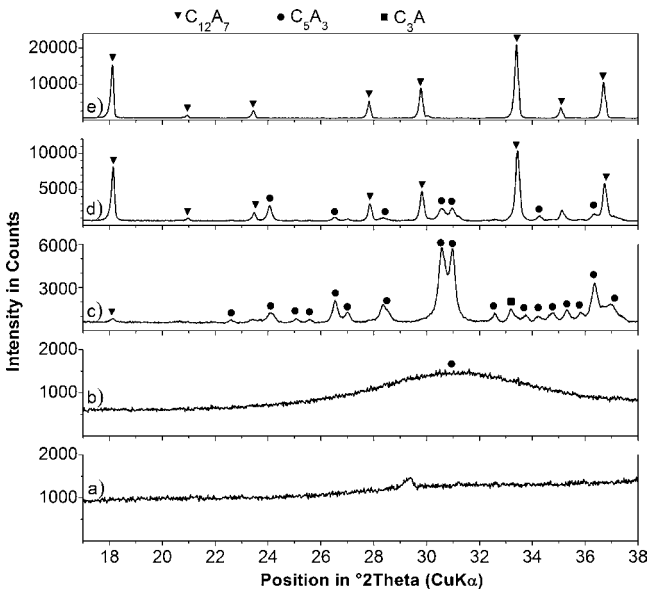

Fig. 1. Phase development of X-ray amorphous precursor powders synthesized by the GNP and sintered in following steps: (a) 298 K; (b) 2 h at 1073 K; (c) 2 h at 1173 K; (d) 2 h at 1273 K; and (e) 2 h at 1473 K.

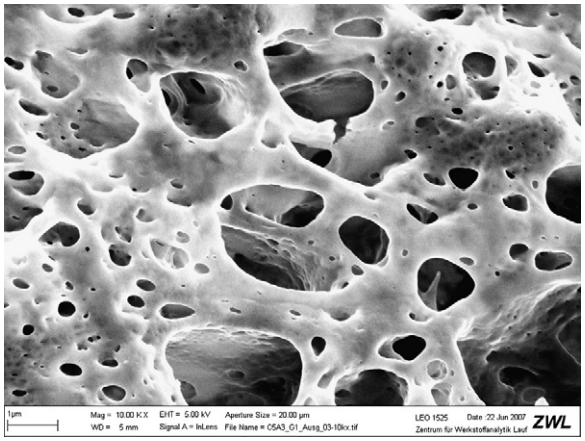

Fig. 2. Amorphous starting material synthesized by GNP corresponding X-ray pattern given in Fig. 1a.

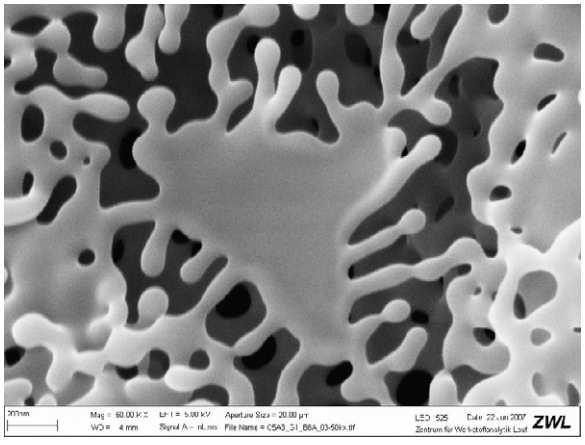

Fig. 3. Precursor powder of the GNP sintered 2 h at 1073 K, corresponding X-ray pattern given in Fig. 1b.

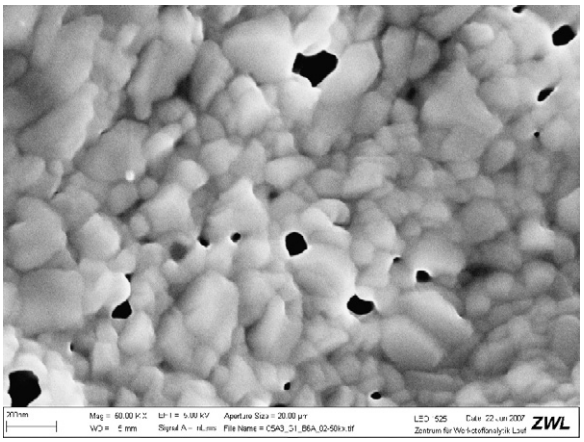

Fig. 4. C_5A_3 (+small amounts of C_3A) produced by sintering the precursor powder (GNP) for 2 h at 1173 K, corresponding X-ray pattern given in Fig. 1c.

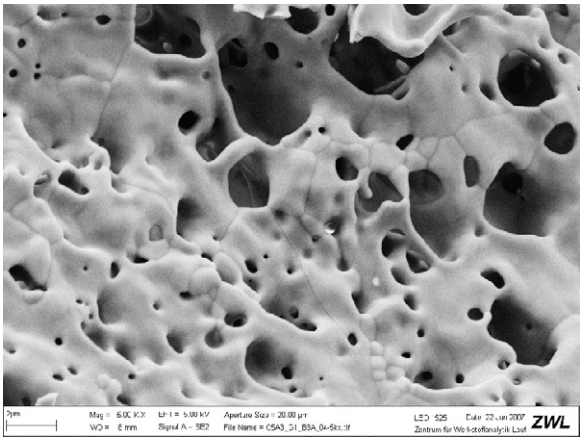

Fig. 5. Pure $C_{12}A_7$ produced by sintering the precursor powder (GNP) for 2 h at 1473 K, corresponding X-ray pattern given in Fig. 1e.

done using the fundamental parameter approach [33]. By assuming spherical crystallites an average crystallite size of 43 nm was calculated. Sintering the powder 2 h at 1273 K the amounts of C_5A_3 and C_3A decrease and the stable phase $C_{12}A_7$ occurs (Fig. 1d). Using a temperature of 1473 K (2 h) the reaction is complete and pure $C_{12}A_7$ was obtained (Fig. 1e). The maximum grain size is below 3 μm and a foamy structure is obtained after the final sintering step (Fig. 5). The phase formation of precursor powders synthesized by polymer precursor method is similar – also C_5A_3 occurs at 900 °C. For the complete conversion of C_5A_3 to $C_{12}A_7$ also a sintering step of 2 h at 1473 K is necessary. The particle size of this $C_{12}A_7$ is slightly smaller, but the particles are more agglomerated. The specific surfaces of the pure $C_{12}A_7$ powders synthesized by the three different synthesis methods are given in Table 1.

Homogenization of the raw materials using GNP and Pechini method yields calcium aluminates at 1173 K. At these temperatures, the metastable phase C_5A_3 occurs instead of stable $C_{12}A_7$. To produce crystalline $C_{12}A_7$, higher temperatures than 1273 K are

Table 1
Specific surfaces of $C_{12}A_7$ produced by different synthesis methods.

$C_{12}A_7$	Glycine nitrate process	Polymer precursor synthesis	Solid state reaction
BLAINE (cm^2/g)	4855	2972	1350
BET (m^2/g)	1.26	1.47	0.28

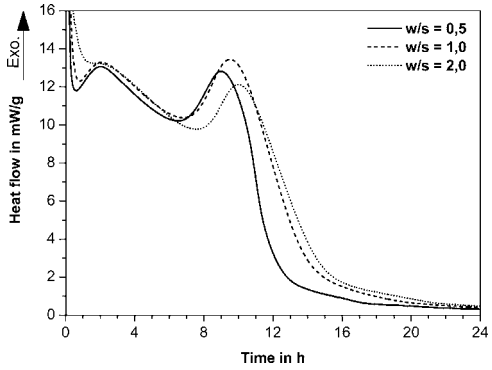

Fig. 6. Heat flow from the hydration of $C_{12}A_7$ (solid state reaction) at various w/s ratios, T = 293 K.

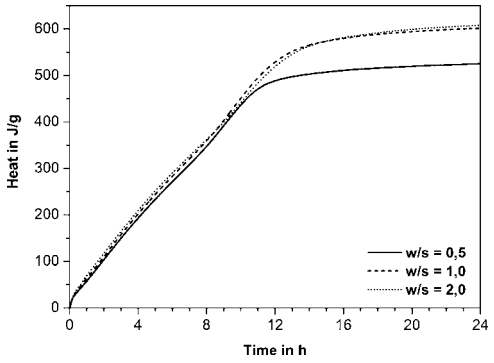

Fig. 7. Total heat liberation from the hydration of $C_{12}A_7$ (solid state reaction) at various w/s ratios (0.5, 1.0 and 2.0), T = 293 K.

necessary. To get pure phases at adequate sinter times for both methods are at least 2 h at 1473 K necessary. Nevertheless, the handling of the Pechini method is much easier because it is more difficult to control the combustion reaction of the GNP. The particle sizes of the samples obtained by the two low temperature synthesis methods are about 1 μm and the powders are very homogenous. In Table 1 the specific surface measured by BLAINE and BET is given.

3.2. Hydration

$C_{12}A_7$ powders produced by these three synthesis methods were hydrated at 283 K, 288 K, 293 K, 298 K and 301 K. The hydration behaviour was followed by heat flow calorimetry (exothermic reactions). Hydrating powders with high specific surfaces using the injection method the use of a higher water-to-solid (w/s) ratio is necessary. Experiments with $C_{12}A_7$ powders produced by GNP and polymer precursor synthesis showed, that a w/s ratio of 2 is necessary in order to get paste like samples and to ensure that enough water is available at the beginning of hydration reactions. In order to compare all measurements a w/s ratio of 2 was used also for the $C_{12}A_7$ powder produced by the solid state reaction.

The influence of different w/s ratios to $C_{12}A_7$ powders produced by solid state reaction is shown in Fig. 6. Consequently, a higher w/s ratio yields to a light delayed second hydration reaction. The total amount of heat does not differ for different w/s ratios of 1 and 2 (Fig. 7).

In Fig. 8a the heat flow diagrams for $C_{12}A_7$ produced by solid state reaction are shown at various temperatures. At lower temperatures, the maximum heat flow of the first calorimetric peak decreases and the maximum heat flow of the second calorimetric peak increases. The strongest retardation of the second hydration maximum is observed at a temperature of 288 K. The calculated heat liberations of these measurements are lower at lower temperatures at the beginning of the hydration reaction (0–15 h) (Fig. 9a). After 15 h of hydration, the hydration reaction is accelerated at lower hydration temperatures. Finally, the heat of evolution is the strongest at the lowest hydration temperature of 283 K.

Heat flow (Fig. 8b and c) and heat of formation (Fig. 9b and c) diagrams of $C_{12}A_7$ powder, produced by the GNP and the polymer precursor method show a comparable tendency in terms of hydration behaviour in comparison to $C_{12}A_7$ powders produced by the solid state reaction. As a difference, the maximum heat flows and heats are much higher and all reactions are accelerated. Additionally, the maximum of the second hydration peak is most delayed at a temperature of 293 K (Fig. 8b and c). The most reactive $C_{12}A_7$ was produced by the GNP.

In addition to calorimetric studies the hydration products were measured by X-ray diffraction after 50 h hydration starts. At 283 K, 288 K and 293 K the hydrate phases C_2AH_8 and very small amounts of CAH_{10} und $C_2AH_{7.5}$ were identified. At 298 K only C_2AH_8 occurs and at 301 K additionally small amounts of hydrogarnet can be detected. In the hydrated $C_{12}A_7$ powders, produced by the solid state reaction, additional unreacted $C_{12}A_7$ is still present after 50 h of hydration. The $C_{12}A_7$ powders produced by GNP and polymer precursor synthesis are completely hydrated at that time. In all samples, very small amounts of hemi carbonate $C_3A(CH)_{0,5}(Cc)_{0,5}H_{11,5}$ can be detected, caused by CO_2 uptake from air.

SEM investigations of hydrated powders were made 2 h after the addition of water. Fig. 10 shows the hydrated powder synthesized by the GNP. The small grains are covered by a hydrate shell (Fig. 10a). Precipitations occurring through the freezing process can be seen (Fig. 10b). On the right side (c) the first hydration products occurred (Fig. 10c). The shells seem to retard the dissolving process of $C_{12}A_7$. In higher magnification of Fig. 11 the dense hydrate shells can be seen. The hydrate shells around the $C_{12}A_7$ produced by the solid state reaction are extremely porous (Fig. 12).

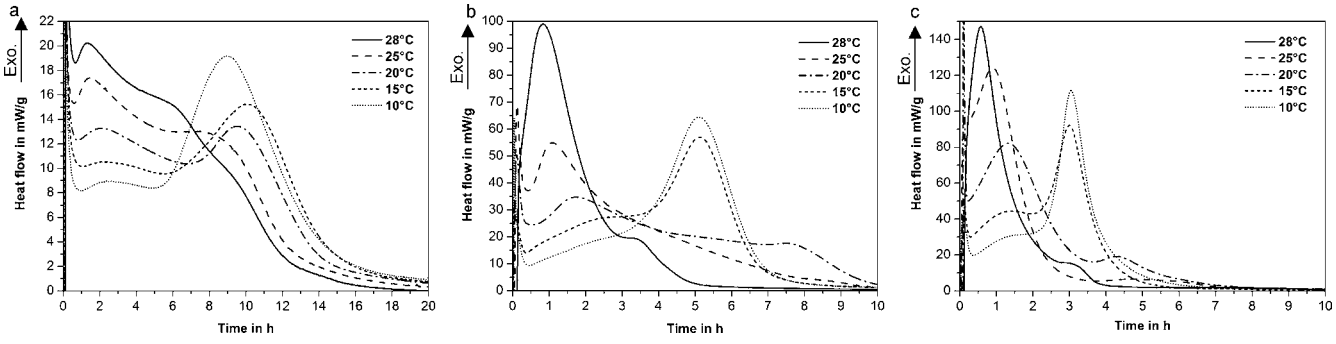

Fig. 8. Heat flow from the hydration of $C_{12}A_7$ produced by solid state reaction (a), polymer precursor synthesis (b) and glycine nitrate process (c) at various temperatures, w/s = 2.

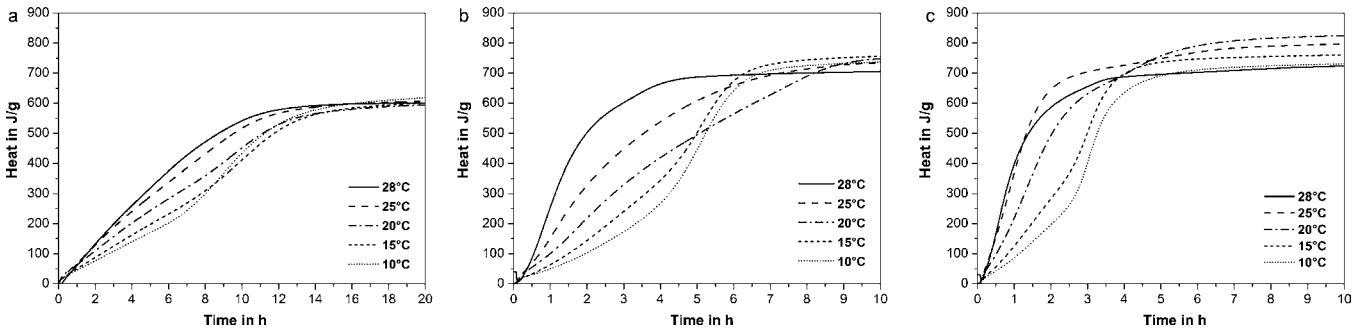

Fig. 9. Total heat liberation from the hydration of $C_{12}A_7$ produced by solid state reaction (a), polymer precursor synthesis (b) and glycine nitrate process (c) at various temperatures, w/s = 2.

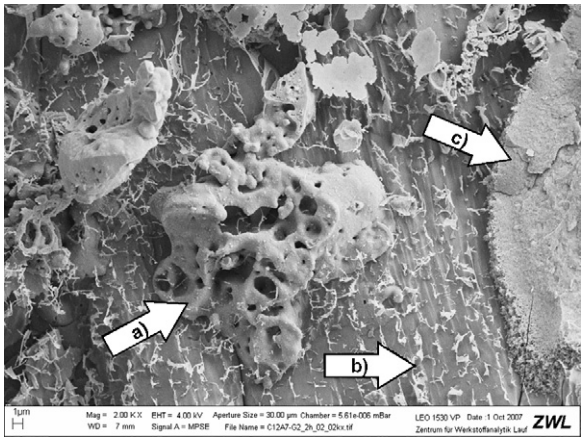

Fig. 10. Cryo-SEM image of $C_{12}A_7$ (GNP) 2 h after the addition of deionised water, w/s = 2, T = 293 K, (a) $C_{12}A_7$ grain covered by hydrate shells, (b) precipitations occurring through the freezing process, and (c) fine crystalline hydration products.

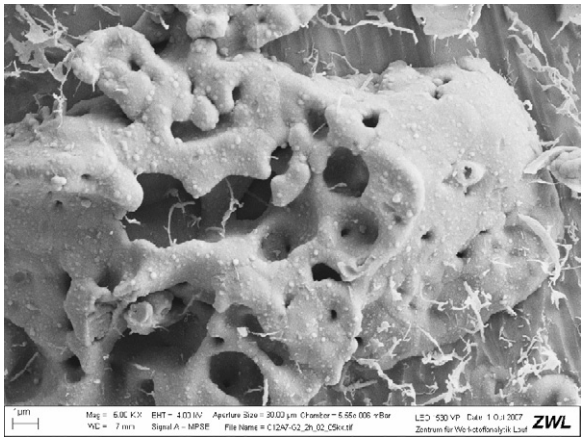

Fig. 11. Cryo-SEM image of fine crystalline dense hydrate shells around a $C_{12}A_7$ grain (GNP), 2 h after the addition of deionised water, w/s = 2, T = 293 K.

Every calorimetric graph of hydrating $C_{12}A_7$ powders shows two peaks and consequently there are two different reactions. According to the literature [24,25] and own investigations the first calorimetric peak corresponds to the formation of hydrate layer around the $C_{12}A_7$ grains. A decrease in the temperature from 301 K to 288 K has a decrease of the maximum heat flow of the first calorimetric peak and less thick and dense layers around the $C_{12}A_7$ grains as consequence. The second calorimetric peak correlates with the further hydration reaction of $C_{12}A_7$ and the formation of lamellar hydrate phases. This reaction is strongly dependant on the first hydration reaction peak. The delay of the second peak in the calorimetric graphs at 288 K (solid state reaction) and 293 K (GNP and polymer precursor synthesis) can be explained with the nucleation problem at these temperature ranges as described by Edmonds and Majumdar [23].

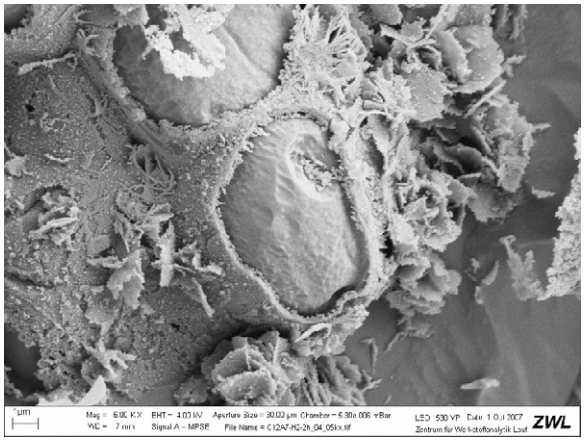

Fig. 12. Cryo-SEM image of coarsely crystalline porous hydrate shells around a $C_{12}A_7$ grain (solid state reaction), 2 h after the addition of deionised water, w/s = 2, T = 293 K.

The cryo-SEM images confirm the theory of forming hydrate layers around the $C_{12}A_7$ grains. Further they showed that the layers produced by hydrating $C_{12}A_7$ powder from solid state reaction are more porous because the powder was sintered by higher temperatures for longer times and this has as a consequence that the surfaces have less defects where solution processes normally start [34].

Comparing the calorimetric graphs of $C_{12}A_7$ at 293 K, produced by the different synthesis methods, the first reaction (building of hydrate shells) is increased by a higher specific surface. The second reaction (further hydration reaction and building of hydrate phases) is accelerated by higher surface areas.

The measurements have shown that the specific surface measured by BLAINE correlates with the hydraulic reactivity measured by heat flow calorimetry.

Acknowledgements

The authors thank the Zentrum fuer Werkstoffanalytik Lauf GmbH for the possibility of using the SEM and M. Fylak for assistance in preparation and handling of the cryo-technique.

References

[1] H. Poellmann, N. Winkler, R. Oberste-Padtberg, R. Meyer, J. Goeske, B. Raab, 28th International Conference on Cement Microscopy, Denver (USA), 2006, pp. 150–187.

[2] H. Poellmann, Calcium Aluminate Cements, IOM Communications Ltd, Edinburgh/UK, 2001, pp. 79-119.
[3] B. Raab, S. Stoeber, H. Poellmann, Calcium Aluminate Cements, Avignon/France, IIHS BRE Press, 2008, pp. 79–92.
[4] A.A. Goktas, M.C. Weinberg, J. Am. Ceram. Soc. 74 (5) (1991) 1066–1070.
[5] L. Kerns, M.C. Weinberg, S. Myers, R. Assink, J. Non Cryst. Solids 232–234 (1998) 86–92.
[6] D. Stephan, P. Wilhelm, Z. Anorg. Allg. Chem. 630 (2004) 1477–1483.
[7] C.-C. Hwang, T.-Y. Wu, J. Wan, J. Mater. Sci. 39 (2004) 4687–4691.
[8] A.C. Tas, J. Am. Ceram. Soc. 81 (11) (1998) 2853–2863.
[9] Y.J. Yang, T.L. Wen, H. Tu, D.Q. Wang, J. Yang, Solid State Ionics 135 (2000) 475–479.
[10] T. Mimani, K.C. Patil, Mater. Phys. Mech. 4 (2001) 134–137.
[11] C.-C. Hwang, T.-Y. Wu, Mater. Sci. Eng. B111 (2004) 197–206.
[12] T. Peng, X. Liu, K. Dai, J. Xiao, H. Song, Mater. Res. Bull. 41 (2006) 1638–1645.
[13] L. Stievano, L.Y. Piao, I. Lopes, M. Meng, D. Costa, J.-F. Lambert, Eur. J. Mineral. 19 (2007) 321–331.
[14] P. Blennow, K.K. Hansen, L.R. Wallenberg, M. Mogensen, J. Eur. Ceram. Soc. 27 (2007) 3609–3612.
[15] G. Kakali, R. Chrysafi, A. Gaki, T. Perraki, A. Tsitouras, 12th International Congress on the Chemistry of Cement, Montreal/Canada, 2007.
[16] A. Gaki, R. Chrysafi, G. Kakali, J. Eur. Ceram. Soc. 27 (2007) 1781–1784.
[17] A. Gaki, T. Perraki, G. Kakali, J. Eur. Ceram. Soc. 27 (2007) 1785–1789.
[18] S.-H. Hong, J.F. Young, J. Am. Ceram. Soc. 87 (7) (1999) 1681–1686.
[19] S.-J. Lee, G.-S. Kim, J. Ceram. Process. Res. 3 (3) (2002) 136–140.
[20] S.-J. Lee, M.-H. Lee, J. Mater. Sci. Lett. 22 (2003) 1291–1293.
[21] Y.L. Chai, D.T. Ray, G.J. Chen, Y.H. Chang, J. Alloys Compd. 333 (2002) 147–153.
[22] A. Douy, M. Gervais, J. Am. Ceram. Soc. 83 (1) (2000) 70–76.
[23] R.N. Edmonds, A.J. Majumdar, Cem. Concr. Res. 18 (1988) 473–478.
[24] Y. Qijun, F. Xiuji, S. Shuichi, 10th International Congress on the Chemistry of Cement, Gothenburg, 1997, 2ii043–8 pp.
[25] K.-S. You, J.-W. Ahn, K.-H. Lee, S. Goto, Cem. Concr. Comp. 28 (2006) 119–123.
[26] M. Fylak, J. Göske, W. Kachler, R. Wenda, H. Pöllmann, Microsc. Anal. 102 (2006) 9–12.
[27] H. Pöllmann, H.J. Kuzel, H.W. Meyer, 13th International Conference on Cement Microscopy, Florida, USA, 1991, pp. 303–313.
[28] M. Schmidt, H. Pöllmann, Calcium Aluminate Cements, Avignon, IHS BRE Press, 2008, pp. 93–108.
[29] S. Brunauer, P.H. Emmett, E. Teller, J. Am. Ceram. Soc. 60 (2) (1938) 309–319.
[30] E. Aruja, Acta Crystallogr. 10 (1956) 337–339.
[31] M.G. Vincent, J.W. Jeffery, Acta Crystallogr. B34 (1978) 1422–1428.
[32] A.R. Stokes, A.J.C. Wilson, Math. Proc. Camb. Phil. Soc., Cambridge University Press, 1942, pp. 313–322.
[33] R.W. Cheary, A.A. Coelho, J.P. Cline, J. Res. Natl. Inst. Stand. Technol. 109 (2004) 1–25.
[34] A.C. Lasaga, A. Lüttge, Eur. J. Mineral. 15 (2003) 603–615.